Swift electrochemical detection of paraben an endocrine disruptor by In_2O_3 nanobricks

Swift electrochemical detection of paraben an endocrine disruptor by In_2O_3 nanobricks

Swift Electrochemical Detection of Paraben an Endocrine Disruptor By In_2O_3 Nanobricks

Ahsanulhaq Qurashi[a], Jahangir Ahmad Rather[b,d], Toshinari Yamazaki[c], Manzar Sohail[a]*

Karolien De Wael[b] , Belabbes Merzougui[a], Abbas Saeed Hakeem[a],

[a]*Center of Research Excellence in Nanotechnology and Department of Chemistry, King Fahd University of Petroleum & Minerals Dhahran 31261, Saudi Arabia*

[b]*University of Antwerp, Department of Chemistry, Groenenborgerlaan, 171, B–2020, Antwerp, Belgium*

[c] *Department of Engineering, Toyama University, 3190 Gofuku, Toyama 930-8555, Japan*

[d]*Department of Chemistry, Sultan Qaboos University, Box 36, Al-Khod 123, Oman*

Abstract

Novel indium oxide (In_2O_3) nanobricks have been prepared by template-less and surfactant-free hydrothermal synthesis method and were characterized by X-ray diffraction (XRD), Raman spectroscopy, Photoluminescence (PL) spectroscopy and field emission scanning electronic microscopy (FESEM). The synthesized In_2O_3 nanobricks were successfully immobilized on the surface of glassy carbon electrode for the detection of *Parabens* (butylparaben). Owing to the unique structure and intriguing properties of these In_2O_3 nanobricks, the nanostructured thin-film electrode has shown an obvious electrocatalytic activity for the detection of butylparaben (BP). The detection limit (LOD) was estimated as 3s/m and the sensitivity (LOQ) was calculated as 10 s/m and were found to be 0.08 μM and 0.26 $\mu A n M^{-1} cm^{-2}$ respectively. This sensor showed high sensitivity compared with the reported electrochemical sensors for the detection of BP. The fabricated sensor was successfully applied for the detection of butyl paraben in real cosmetic samples with good recovery ranging from 96.0% to 100.3%.

Keywords: In_2O_3 nanobricks, synthesis, Electrochemical BP detection

[*]*Corresponding author email: ahsanulhaq06@gmail.com*

Tel: 00966-03-860-7063

1. Introduction

Indium oxide (In_2O_3) nanostructures are n-type semiconductors having wide band gap (*ca*.3.6 eV) and are extensively explored in recent years due to their excellent electronic and optical properties in optoelectronic devices, solar cells, gas sensors and biosensors [1, 2]. Up to now, various methods (vapor transport and wet chemistry) have been employed for the synthesis of In_2O_3 nanostructures [3, 4]. Compared with the vapor transport methods, the solution based hydrothermal synthesis is demonstrated to be environmentally benevolent and is able to produce In_2O_3 nanostructures in large scale which includes quantum dots, nanowires, nanotubes and 3-D assembled nanostructures [5]. In_2O_3 nanostructures have been immensely used for detecting various chemical species (C_2H_5OH, HCHO and NH_3) due to their improved sensing properties [6–9].

The European Commission during the conference in June 2012, on "Endocrine Disruptors (EDCs): Current challenges in science and policy" listed Parabens as category 1 priority phenolic endocrine disruptor substances, based on evidence that they obstruct hormonal functioning. Parabens are designed as esters of p-hydroxybenzoic acid and are extensively used as antimicrobial preservatives in food ingredients, cosmetic products (deodorants, antiperspirents, skin moisturizes, body creams, body sprays and suncare) as well as pharmaceutical preparations. The parabens present in these products are incessantly released into the aquatic media by domestic wastewater. Therefore, there is growing concern in relation to their potential long-term effects on humans and wild life [10–14].

Literature survey reveals various techniques for parabens detection, such as high performance liquid chromatography [15], capillary electrochromatography [16], gas chromatography [17], flow injection system combined with chemiluminescence [18], solid phase extraction (SPE) and supercritical fluid extraction (SFE) [19, 20]. Although these techniques have high accuracy with low detection limits, but they are expensive, time-consuming and due to the intricacy of the environmental matrices, pre-concentration of the samples are needed for the analysis [21]. Electrochemical sensors with potential for environmental applications have been a subject of tremendous interest in recent past [22–24]. Recently nanostructured electrodes attracted huge attention for ultrafast phenolic compound detection [25, 26]. The present work describes an unpretentious method based on a thin film electrode consisting of synthesized In_2O_3 nanobricks coated on glassy carbon electrode (GCE) for the detection of trace amounts of BP. This thin film

electrode showed an exceptional electrocatalytic activity due to significant drop in the anodic overpotential and notable improvement of the anodic current of BP compared with the electrochemical performances obtained at a GCE.

2. Experimental

2. 1 Synthesis of In_2O_3 nanobricks

The typical experiment for the synthesis of In_2O_3 nanobricks involves a 100 mL capacity autoclave with a Teflon liner filled with $InCl_3.4H_2O$ (0.5 mM) dissolved in distilled water (100 mL). Then, hexamethylene tetramine (HMTA) (10 mM) was added into the autoclave and the reactive mixture was stirred robustly for 30 min. After stirring autoclave was sealed and upheld at 150 °C for 14 h in an oven. Then autoclave was cooled down to room temperature naturally and the light yellow sample was collected and washed several times with ethanol, acetone and distilled water to eliminate the probable residual ions in the sample. The products were dried in a vacuum at 80 °C for 4 h and calcined at 400°C to obtain In_2O_3 nanobricks.

3. Results and Discussion

The crystalline structure of the synthesized indium oxide nanobricks was investigated by X-ray diffraction (XRD) (Shimadzu XRD 6100 Cu Kα (0.15419 nm) technique (Figure 1). All the peaks were indexed to the pure cubic phase with lattice parameter a = 1.011Å (JCPDS No. 89–4595), indicating that pure cubic phase of In_2O_3 is obtained. The synthesized indium oxide nanobricks were also characterized by Raman spectroscopy and Photoluminescence (PL) spectroscopy, which indicates high crystallinity with a large amount of oxygen deficiency of cubic In_2O_3 nanobricks (Supporting information).

Surface morphological features of indium oxide nanobricks were investigated by field emission scanning electronic microscope (FESEM) equipped with EDX. Figure 1B (a-d) shows various FESEM magnification micrographs of In_2O_3 nanobricks. A panoramic view of FESEM micrographs shows that the sample consists exclusively of uniform nanobricks without impurity particles or aggregates. The nanobricks have well defined uniform dimensions with edge length ranges from 400-600 nm and height ranges from 200-250 nm. The top surface shows some cracks at the midst of each box might be caused by mass transport across other side surfaces, which also resulted in fewer nanoparticle formations around each brick. Their edges are sharp and sides and top surface are extremely smooth.

Before sensor fabrication, the GCE surface was polished with PK-4 polishing kit, BASi MF-2060 consecutively followed by washing systematically with redistilled deionized water until a mirror like finish was obtained. It was then dipped in a beaker containing 0.2 mol/L H_3PO_4 solutions to remove the adhered powder, rinsed with distilled water and dried at room temperature for 10−15 minutes. Stock solution of indium oxide nanobricks in form of an ink (1.0 mg/mL) was prepared in 50% dimethyl sulfoxide (DMSO) by ultrasonication for 30 minutes. Then 8 µL of this solution was deposited onto the surface of GCE using a microsyringe and dried under IR lamp.

Electrochemical measurements were performed using a µ–Autolab Potentiostat/Galvanostat PGSTAT from Metrohm (Netherlands), integrated with a PC provided with the NOVA 1.8 software. A three-electrode cell was used which consists of In_2O_3/GCE as working electrode, Ag/AgCl as reference electrode and a graphite rod as an auxiliary electrode. All working solutions for electrochemical measurements were de-aerated for 10-15 min. with purified nitrogen gas. All pH–metric measurements were made on a Decible DB–1011 digital pH meter fixed with a glass electrode and a saturated calomel electrode as reference, which was previously standardized with buffers of known pH [27].

The electrode fabrication was characterized by electrochemical impedance spectroscopy (EIS) and cyclic voltammetry (CV). Nyquist plot of EIS shows semicircle part and diameter of semicircle equals the charge-transfer resistance (R_{ct}). The R_{ct} value for the 1.0 mM $K_3Fe(CN)_6^{3-/4-}$ redox probe obtained at In_2O_3/GCE was 195Ω (Figure 1C (curve c) was less than 686Ω Figure 1C (curve b) achieved at GCE implied that charge transfer resistance of the electrode surface decreased and the charge transfer rate increased on the fabrication of sensor. This may be due to high conductivity and large surface area of the In_2O_3 nanobricks at the surface of GCE. This assumption was further verified by studying the cyclic voltammetry (CV) of redox probe $K_3[Fe(CN)_6]$ to characterize the property of modified electrode. Figure 1D shows the CVs obtained at bare GCE (curve b), In_2O_3/GCE, (curve c) in 1.0 mM $K_3[Fe(CN)_6]$. The apparent microscopic areas of these modified electrodes was calculated using Randles-Sevcik equation; $i_p = (2.69 \times 10^5)\, n^{3/2} AC_0 {}^*D_0{}^{1/2} \nu^{1/2}$. Where I_p = current maximum in amps, n = number of electrons transferred in the redox event, A = electrode area in cm^2, F = The Faraday Constant in C moL^{-1}, D = diffusion coefficient in cm^2/s, C = concentration in moL/cm^3 and υ = scan rate in V/s. For $K_3[Fe(CN)_6]$; n = 1 and D = 7.6×10^{-6} cm^2/s and the microscopic areas of GCE and In_2O_3/GCE was calculated and was found to be (0.02 cm^2) and (0.042 cm^2) respectively. Evidently, the In_2O_3

modified electrode (In_2O_3/GCE) had almost twice the surface area compared to GCE and thus acts as a better electrocatalyst for the oxidation of BP. Furthermore, negative shift in peak position of Fe^{II} oxidation reveals fast charge transfer on In_2O_3/GCE, which is same in accordance with EIS observation.

Figure 1

The electrocatalytic activity of In_2O_3/GCE sensor for the oxidation of 2.4 μM BP (0.1 mM BP stock solution in ethanol; BP was purchased from Sigma-Aldrich, Belgium) was studied in phosphate buffer (pH 7.0) by cyclic voltammetry. A typical CV of BP exhibits a single well-defined anodic peak at 0.85 V (vs. Ag/AgCl) assigned to the oxidation of phenolic (OH) group and no corresponding cathodic peak was obtained indicating the irreversibility of electrode process. The mechanism involves single electron oxidation of phenolic group (OH) of BP, which results in formation of benzoquinone (Scheme 1). It was also observed that modification of GCE surface by a thin film of In_2O_3 remarkably improved the sensitivity of In_2O_3/GCE towards the BP detection. The reason for better performance of In_2O_3/GCE sensor may due to the nanometer dimensions of In_2O_3, electronic structure, topological and high surface area of In_2O_3 nanostructured thin film. Figure 2 illustrates the voltammograms, CV (Figure 2A) and SWV (Figure 2B) of 2.4 μM BP at a bare GCE and In_2O_3/GCE and it is clear that fabricated In_2O_3/GCE sensor increase the oxidation peak current of BP and also results in decrease of the over potential. This confirms the electrocatalytic effect of In_2O_3/GCE for faster and better detection of BP.

Scheme 1

Figure 2

The quantitative analysis of BP using In_2O_3/GCE was performed by squarewave voltammetry (SWV). The SWV peak current was measured as a function of BP concentration at least three times under the optimized operational parameters (Figure 3). The calibration plot of concentration versus peak current was found to be linear over the range of 0.14 μM to 2.4 μM. The detection limit (LOD) was estimated as 3s/m and found to be 0.08 μM and the sensitivity (LOQ) was calculated as10s/m and was found to be 0.26 $\mu A n M^{-1} cm^{-2}$ (s representing the standard deviation of the peak currents (n = 3) and m is the slope of the calibration curve).

Figure 3

The validation of the developed In_2O_3/GCE sensor was carried out to evaluate the selectivity and specificity in presence of some potential interfering substances having similar structure as BP. Under optimal conditions, the interference test was performed in the presence of 100–fold concentration of various endocrine disruptors' viz., phenol, and bisphenol-A. The results obtained indicates that they do not interfere on the signals of 2.4 µM BP with RSD value of 3.5% indicates that the fabricated sensor is suitable for detection of BP. The In_2O_3/GCE sensor showed good stability and reproducibility for the detection of BP (Supporting information).

The real sample analysis for the detection of BP was done by analysis of commercial product *True match cream ® (LOREAL).* A 0.1 g of cream was dissolved in 25 mL of ethanol by ultrasonic agitation for 30 min and then the sample solution was centrifuged for 10 min in order to remove the excipients and finally transferred into 100 volumetric flask and make up with phosphate buffer of pH 7.0 to obtain 10 mg mL^{-1} solution of cosmetic sample. The amount of BP present in the cream was determined by standard addition method at the developed sensor In_2O_3/GCE. According to the peak current, the total concentration of BP was calculated with an average regression equation, which was found to be 0.53 µM in this 10 time diluted sample (equilent to 5.3 µM , 0.12%) and is within the permissible limit of 0.19 % BP in cosmetics according to the European scientific committee (SCCS) on consumer safety on 22 March 2011 (SCCS/1348/11). The reliability of the proposed method was verified by calculating the recovery by standard addition method using three different standard samples (0.5, 1.0 and 1.5 µM). The average recovery was obtained in the range of 95.8% to 108.5% with the RSD value less than 5% (Table 1) indicates high accuracy and precision of the developed method for the determination of BP in cosmetic samples.

Table 1

4. Conclusion

The present study reports synthesis of the In_2O_3 nanobricks by simple and low temperature hydrothermal method and characterized by FESEM and XRD techniques. A versatile electrochemical sensor was developed based on deposition of In_2O_3 nanobricks on GCE for the detection of BP and its analytical performance was relatively studied with bare GCE. The

obtained results show that a nanocomposite film of In_2O_3 nanobricks provided notable advantages over GCE in accomplishing faster response, tremendous electrocatalytic activity, superior repeatability, lower background current, and low detection limit, which could be accredited to its larger specific surface area and greater electron transfer rate. The detection limit (LOD) and sensitivity (LOQ) was found to be 0.08 μM and 0.26 $\mu A n M^{-1} cm^{-2}$ respectively. This developed sensor becomes an on-field realistic device for expedient detection of other phenolic endocrine disruptors in ecological matrices.

5. References

[1] G. Shen, B. Liang, X.Wang, H. Huang, D. Chen, Z. L. Wang, Ultrathin In_2O_3 nanowires with diameters below 4 nm: synthesis, reversible wettability switching behavior, and transparent thin-film transistor applications, ACS Nano 5 (2011) 6148–6155.

[2] R. Yousefi, B. Kamaluddin, Room-temperature PL spectra indicate that they have a potential application as properties of ZnO nanobelts, Appl. Surf. Sci. 255 (2009) 9376–9380.

[3] A. Vomiero, S. Bianchi, E. Comini, G. Faglia, M. Ferroni, N. Poli, G. Sberveglieri, Nanobelts of Semiconducting Oxides, Thin Solid Films 515 (2007) 8356–8359.

[4] Z. W. Pan, R.Z. Dai, Z.L. Wang, Gas Sensing with Nano-Indium Oxides (In2O3) Prepared via Continuous Hydrothermal Flow Synthesis, Science 291(2001)1947–11947.

[5] W. J. Kim, D. Pradhanb Y. Sohn, Fundamental nature and CO oxidation activities of indium oxide nanostructures: 1D-wires, 2D-plates, and 3D-cubes and donuts, J. Mater. Chem. A 1(2013)10193–10202.

[6] H. Jiang, J. Hu, F. Gu, W. Shao, C. Li, Synthesis and Photocatalytic Properties of a Polyaniline-Intercalated Layered Protonic Titanate Nanocomposite with a p−n Heterojunction Structure, Chem. Commun. 90 (2009) 3618–3620.

[7] N. D. Singh, C. Y. Yan, P. S. Lee, Chemical sensing investigations on Zn–In_2O_3 nanowires, Sens. Actuators B 150 (2010) 19–24.

[8] J. X. Wang, B. Zou, S. P. Ruan, J. Zhao and F. Q. Wu, Synthesis, characterization, and gas-sensing property for HCHO of Ag-doped In_2O_3 nanocrystalline powder, Mater. Chem. Phys. 117 (2009) 489–493.

[9] B. X. Li, Y. Xie, M. Jing, G. X. Rong, Y. C. Tang, G. Z. Zhang, In_2O_3 hollow microspheres: Synthesis from designed in (OH)(3) precursors and applications in gas sensors and photocatalysis, Langmuir 22 (2006) 9380–9385.

[10] A. Hossaini, J. J. Larsen, J. C. Larsen, Lack of oestrogenic effects of food preservatives (parabens) in uterotrophic assays, Food Chem. Toxicol. 38(2000) 319–323.

[11] P.D. Darbre, J. R. Byford, L. E. Shaw, S. Hall, N. G. Coldham, G. S. Pope, Concentrations of parabens in human breast tumours, J. Appl. Toxicol. 23 (2003) 43–51.

[12] S. Oishi, Decreased excretion of testosterone and alterations in the male reproductive tract were observed in male rodents after exposure to butyl and propyl parabens but not to methyl and ethyl parabens, Arch. Toxicol. 76 (2002) 423–429.

[13] J. P. Routledge, J. Odum, J. P. Sumpter, Some alkyl hydroxy benzoate preservatives (parabens) are estrogenic, Toxicol. Appl. Pharm. 153(1998) 12–19.

[14] P. W. Harvey, D. J. Everett, Significance of the detection of esters of p-hydroxybenzoic acid (parabens) in human breast tumours, J. Appl. Toxicology 24(2004)1– 4.

[15] M. Thomassin, E. Cavalli, Y. Guillaume, C. Guinchard, Application of a capillary electrophoresis method for simultaneous determination of preservatives in pharmaceutical formulations, J. Pharm. Biomed. Anal. 15 (1997) 831–838.

[16] K. D. Altria, J. Bestford, Main component assay of pharmaceuticals by capillary electrophoresis J. Capillary Electrophor. 3 (1996) 13-23.

[17] P. Canosa, D. Perez-Palacios, A. Garrido-Lopez, M.T. Tena, I. Rodriguez, E. Rubi, R. Cela, Pressurized liquid extraction with in-cell clean-up followed by gas chromatography-tandem mass spectrometry for the selective determination of parabens and triclosan in indoor dust, J. Chromatogr. A 1161 (2007) 105–112.

[18] R. K. Kobos, Enzyme-based electrochemical biosensors, Trac-Trend. Anal. Chem. 6 (1987) 6–12.

[19] S. Tuncagil, S. Varis, L. Toppare, Design of a biosensor based on 1-(-4-nitrophenyl)-2,5-di-(2-thenyl)-1H pyrrole, J. Mol. Catal. B: Enzym. 64 (2010) 195–199.

[20] R. Kazandjian, A. Klibanov, Regioselective Oxidation of Phenols Catalysed by Polyphenol Oxidase in. Chloroform, J. Am. Chem. Soc.107(1985) 5448–5450.

[21] C. B. Jacobs, M. J. Peairs, B. J. Venton, Carbon nanotube based electrochemical sensors for biomolecules, Anal. Chim. Acta 662(2010) 105–127.

[22] B. J. Sanghavi, W. Varhue, J. L. Chávez, C. Chou, N. S. Swami, Electrokinetic Preconcentration and Detection of Neuropeptides at Patterned Graphene-Modified Electrodes in a Nanochannel, Anal. Chem. 86 (2014) 4120–4125.

[23] B. J. Sanghavi, S. Sitaula, M. H. Griep, S. P. Karna, M. F. Ali, N. S. Swami, Real-Time Electrochemical Monitoring of Adenosine Triphosphate in the Picomolar to Micromolar Range Using Graphene-Modified Electrodes, Anal. Chem. 85 (2013)8158–8165.

[24] B. J. Sanghavi, O. S. Wolfbeis, T. Hirsch, N. S. Swami, Nanomaterial-based electrochemical sensing of neurological drugs and neurotransmitters, Microchim. Acta 182 (2015)1–41.

[25] F. Liu Y. Piao J. S. Choi T. S. Seo, Three-dimensional graphene micropillar based electrochemical sensor for phenol detection, Biosens. Bioelectron 50 (2013)387–392.

[26] C. Carmen M. Mayorga, L. Hlavata, S. Miserere, A. López-Marzo, J. Labuda, J. Pons, A.Merkoçi, Bismuth nanoparticles for phenolic compounds biosensing application, Biosens. Bioelectron. 55 (2014) 3553–59.

[27] A. Qurashi**,** J.A. Rather**,** K. DeWael**,** B. Merzougui**,** N. Tabet and M. Faiz, Rapid microwave synthesis of high aspect-ratio ZnO nanotetrapods for swift bisphenol A detection, Analyst 138 (2013) 47644–768.

Figure and table captions

Figure 1: (A) XRD spectrum of In_2O_3 nanobricks, (B) low and high magnification FESEM images of In_2O_3 nanobricks, (C) Nyquist plots (Inset: Randles equivalent circuit of the GCE and In_2O_3/GCE to fit the impedance data) and (D) cyclic voltammograms of 1.0 mM $K_3[Fe(CN)_6]$ obtained at GCE (curve b) and In_2O_3/GCE, (curve c); scan rate of 20 mVs^{-1}.

Figure 2: (A) Cyclic voltammetric and (B) Squarewave voltammetric behavior obtained at (a) Blank, (b) 2.4 µM BP at GCE and (c) 2.4 µM BP at In_2O_3/GCE; scan rate 20 mVs^{-1}.

Scheme 1: Mechanism of the oxidation of BP at In_2O_3/GCE sensor.

Figure 3: Linearity of squarewave voltammetric peak current of different concentrations of BP at In_2O_3/GCE, (a) Blank (b) 0.14 µM (c) 0.39 µM (d) 0.78 µM (e) 1.04 µM (f) 1.45 µM (g) 1.98 µM (h) 2.4 µM ; Inset a calibration graph represents the variation of current with the concentration of BP. The error bars shows the standard deviation obtained for three separate experiments.

Table 1: Recovery studies of BP by standard solutions in cosmetics using fabricated sensor (n=3)

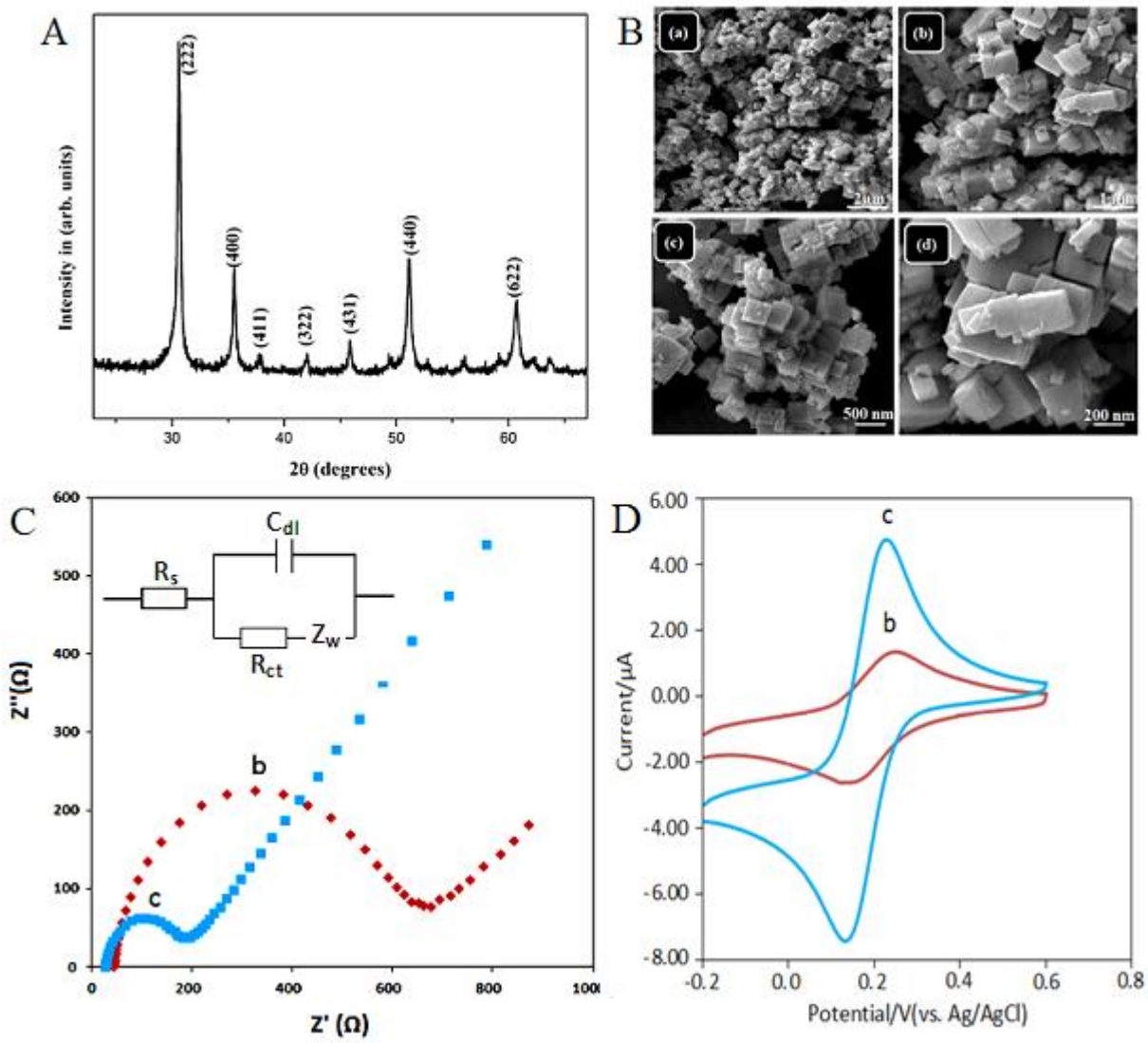
A
(222)
(400)
(411)
(322)
(431)
(440)
(622)
Intensity in (arb. units)
30
40
50
60
2θ (degrees)
B
(a)
(b)
(c)
(d)
500 nm
200 nm
C
C_{dl}
R_s
Z_w
R_{ct}
Z''(Ω)
Z' (Ω)
b
c
D
c
b
Current/μA
Potential/V(vs. Ag/AgCl)

Figure 1

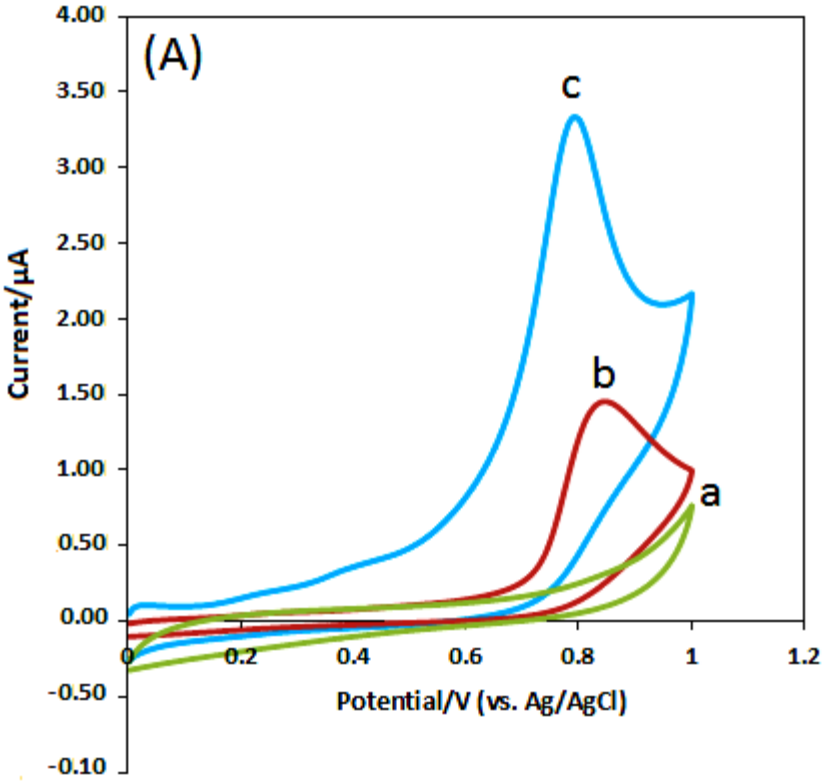

363

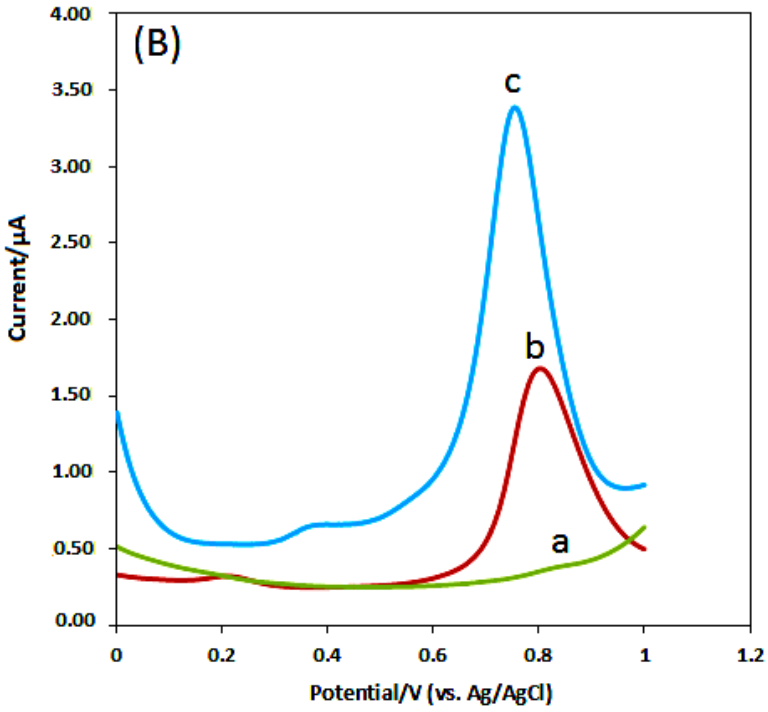

364

365

366 **Figure 2**

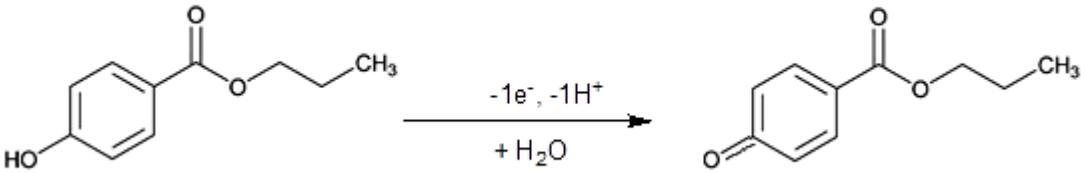

Scheme 1

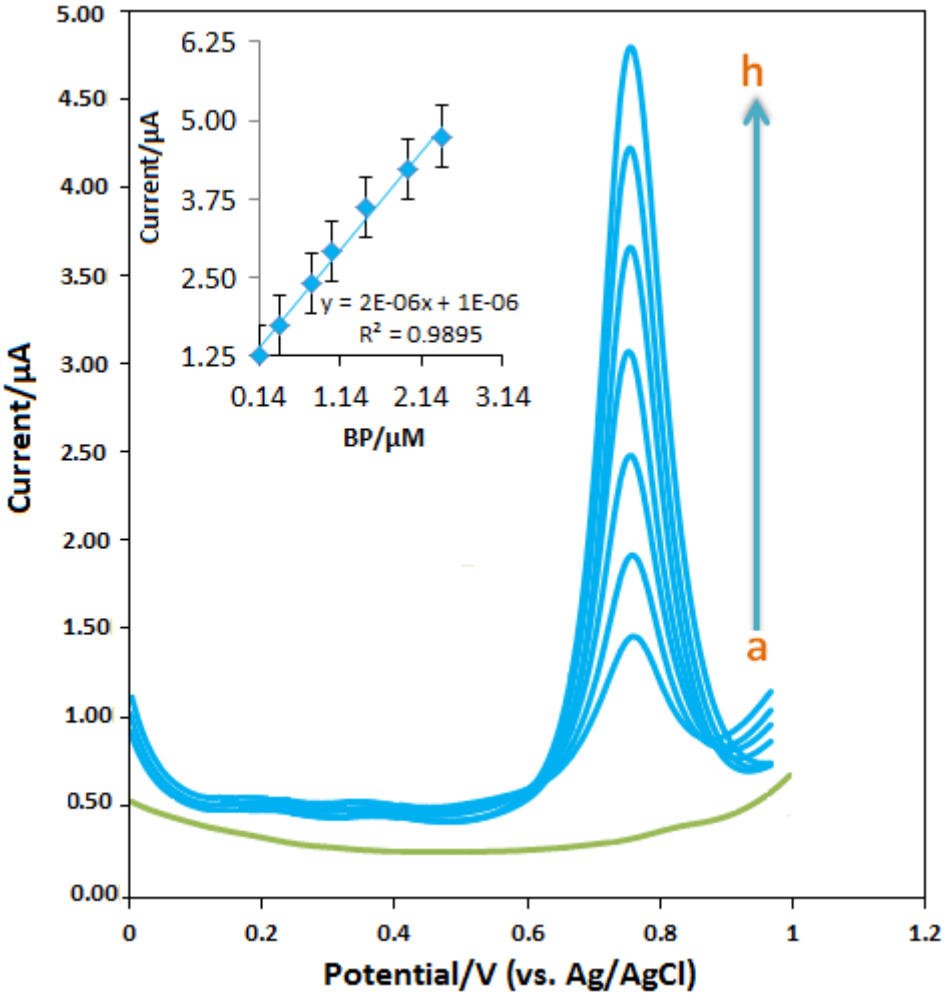
Current/µA
Potential/V (vs. Ag/AgCl)
h
a
Current/µA
BP/µM
y = 2E-06x + 1E-06
R² = 0.9895

Figure 3

406 **Table 1**

Sample	Added (µM)	Found[a] (µM)	Actual (µM)	RSD %	Recovery %
True match Cream	0	0.512	--	2.2	---
True match Cream	0.5	0.970	1.012	3.4	95.8
True match Cream	1.0	1.461	1.512	3.1	96.6
True match Cream	1.5	2.185	2.012	4.9	108.5

407 [a]average of three replicates

408

409